

# Preparation of blend hydrophilic PSF-SPEEK ultrafiltration membranes for oily wastewater treatment

Amir Mansourizadeh\*, Mehrsa Mohammadi

Department of Chemical Engineering, Gachsaran branch, Islamic Azad University, Gachsaran, Iran

## ARTICLE INFO

### Article history:

Received: November 01, 2018

Accepted: December 25, 2018

### Keywords:

Blend PSF hollow fiber membrane  
Sulfonated poly(ether ether ketone)  
Oil rejection  
wastewater treatment

\* Corresponding author

E-mail:

a.mansourizadeh@yahoo.com

Tel.: +98 917 8508373

Fax: +98 74 32332033

## ABSTRACT

Membrane separation is known as an efficient technique for the oily wastewater treatment. Therefore, in the present study, sulfonated poly(ether ether ketone) (SPEEK) was introduced into the polysulfone (PSF) solution in order to enhance the hydrophilicity and the membrane structure for the oil-water separation. The hollow fiber membranes were fabricated via a phase-inversion process. The membranes were characterized by a N<sub>2</sub> permeation test, overall porosity, water contact angle, pure water flux and scanning electron microscopy (SEM) analysis. The blend PSF-SPEEK membrane presented an open finger-like morphology with a thicker outer skin layer and smaller pore sizes. The blend membrane showed overall porosity of 78.8% due to the open structure. The outer surface water contact angle of the blend membrane decreased approximately 8° due to the hydrophilic nature of SPEEK. The blend membrane showed N<sub>2</sub> permeance of 134 GPU and mean pore size of 22 nm. Improved pure water flux of 9.3 L/m<sup>2</sup> h at 400 kPa and the small resistance of 0.483 m<sup>2</sup> h bar/L for the blend membrane were related to the higher hydrophilicity and the open structure. The blend membrane showed the oil rejection of over 98% and the stable water flux of 6.5 L/m<sup>2</sup> h due to the improved structure.

## 1. Introduction

Due to the production of enormous amount of oily wastewater in oil-gas, petrochemical, metallurgical, pharmaceutical and food industries, an efficient separation technology is required to prevent the environmental issues. Membrane separation has been introduced as an efficient technique for the oil-water separation [1–6]. A developed membrane structure is a suitable alternative for the oil separation, where inorganic and polymeric materials are used to prepare the membranes for this purpose [7–10]. Ceramic membranes have demonstrated advantages such as the high mechanical strength and high thermal resistance. However, high cost and the difficulty of fabrication and modification are the negative aspects. On the other hand, due to easy fabrication and modification, high separation efficiency and low cost, polymeric membranes have attracted considerable interest [11–13]. Using highly hydrophilic membranes can cause a decrease in the deposition of the oil on the membrane surface which results in the reduction of membrane fouling and the enhancement of water productivity [14–16]. The ultrafiltration of oil-water emulsions using polysulfone (PSF) membranes were investigated by Chakrabarty et al. [17, 18]. It was found that the addition of polyvinylpyrrolidone (PVP) and polyethylene glycol (PEG) into the polymer solution enhanced the membrane hydrophilicity. Chen et al. [19] produced a novel membrane with two different materials in aspect of hydrophilicity to treat the oil-water emulsion. They grafted polyacrylonitrile (PAN) onto hydrophilic cellulose acetate (CA) by means of free radical polymerization. The results of SEM indicated that the morphology of membrane changed from sponge-like for CA membrane to high finger-like macrovoids for the composite membrane and the flux became about 67 times higher. Zhu et al. [20] synthesized a novel PSF with pendant tertiary amine groups and this functionalized PSF was crosslinked based on a facile reaction between tertiary amine and 1,3-dibromopropane (DBP). The crosslinked PSF and sulfonated poly(ether ether ketone) (SPEEK) were mixed together to fabricate the ultrafiltration membranes by the phase inversion method. The incorporation of highly hydrophilic SPEEK markedly improved the membrane hydrophilicity, surface pore size, permeability, and antifouling properties. The membrane with crosslinked PSF:SPEEK ratio of 1:1 showed the most favorable performance, including almost 3.5 times of pure water flux of the plain PSF membrane and 97% of flux recovery ratio. Saadati and Pakizeh [21] prepared a new PSf/pebax/F-MWCNTs nanocomposite membrane for the nanofiltration of oil/water emulsion. The porous PSF support was prepared and then a thin layer of the pebax as the selective layer was coated on it. By increasing F-MWCNT up to 2 wt%, hydrophilicity, tensile strength and thermal stability significantly improved at pressure range of 10–20 bar. The highest permeate flux was obtained for 0.5 wt% F-MWCNTs loading while the sample containing 2.0 wt% F-MWCNTs showed the best oil rejection. Gao et al. [22] prepared poly(p-phenylene sulfide) (PPS) microporous membrane via a thermally induced phase separation (TIPS), and the superhydrophilic membrane was modified by the nitric acid. A large number of hydrophilic groups, such as –SO–, –SO<sub>2</sub>–, C=O, –NH<sub>2</sub> and –NO<sub>2</sub> groups were introduced onto PPS membrane surface through the interfacial reaction between PPS membrane and HNO<sub>3</sub>. The results indicated that the membrane became superhydrophilic with contact angle of 0° and pure water flux of 154.95 L/m<sup>2</sup> h. The separation performance of the

modified membrane on four different types of oil/water emulsions was studied and all of the separation efficiency were greater than 95%. Zuo et al. [23] prepared poly (vinylidene fluoride) (PVDF) membranes via TIPS method, and surface-modified by polydopamine. The optimal membrane showed a permeation flux of about 2600 L/m<sup>2</sup> h bar for oil/water emulsions (n-hexane, toluene and petroleum ether) accompanied with above 98.5% oil rejections.

Blending with highly hydrophilic polymers can be an alternative to improve the hydrophilicity and the performance of the membranes for the wastewater treatment. SPEEK is a highly hydrophilic polymer due to the sulfone groups. In addition, it is well-known that PSF is a common polymer for the membrane preparation due to its good processibility, excellent mechanical strength, good acidic and alkaline resistance and its high glass transition temperature. However, its low hydrophilic nature can result in severe membrane fouling and the reduction of permeate flux which is a substantial limitation for the practical applications in wastewater treatment.

To the best of our knowledge, the preparation of blend PSF-SPEEK hollow fiber membranes for the oily wastewater treatment has not been previously investigated. In the present study, the ultrafiltration PSF-SPEEK hollow fiber membranes were prepared via a phase inversion process. The membranes were characterized by a gas permeation method, water contact angle and pure water flux. Moreover, the treatment of simulated oily wastewater was conducted through the ultrafiltration system.

## 2. Research Method

### 2.1. Materials

The polysulfone Udel P-1700 in pellet form (Solvay Advance Polymers) was used for the fabrication of the hollow fiber membranes. 1-methyl-2-pyrrolidone (NMP, >99.5%) was supplied by MERCK and used as solvent without further purification. SPEEK as the blend polymer with a degree of sulfonation of 40% was provided by AMTEC, UTM. Kerosene (97% purity, Fluka) was used for the preparation of oil-water emulsion. Its properties are given in Table 1 below.

Table 1. Properties of kerosene used for the preparation of oil-water emulsion

Property	Value
Boiling point range (°C)	175-325
Density (gr/cm <sup>3</sup> )	0.8
Flash point (°C)	>38
Water solubility	slightly
Color	colourless

### 2.2. Preparation and characterization of blend hollow fiber membranes

The PSF polymer (pellet form) was dried at 60±2 °C in a vacuum oven for 24 h to remove the moisture content. The spinning dope solutions of 17 wt.% solid polymer balanced with NMP were prepared (at room temperature 25–27 °C) using stirring until the solution became homogeneous. The second solution containing SPEEK has 10% of the solid polymer. The resulting solutions were degassed for 24 h at room temperature before the spinning. The hollow fiber

spinning process by the dry-jet wet phase inversion was explained elsewhere [24]. Table 2 lists the detailed spinning parameters.

Table 2. Hollow fiber spinning parameters

Dope extrusion (mL/min)	2.0
Bore fluid (mL/min)	0.6
Bore fluid composition (wt.%)	NMP/H <sub>2</sub> O 70/30
External coagulant	Tap water
Air gap distance (cm)	0.0
id/od (mm)	0.3/0.7
Spinning dope temp. (°C)	25
Coagulation bath temp. (°C)	25

Scanning electronic microscopy (SEM) (JEOL JSM-6700F) was used to examine the morphology of the spun PSF hollow fiber membranes. The SEM micrographs of cross-section, external and internal surfaces of the hollow fiber membranes were taken at various magnifications.

The membrane overall porosity is defined as the volume of the pores divided by the total volume of the membrane. The overall porosity ( $\varepsilon_m$ ) was calculated according to the commonly used method based on density measurements [25], as the following equation:

$$\varepsilon_m(\%) = \left[ 1 - \frac{\rho_f}{\rho_p} \right] \times 100 \quad (1)$$

Where  $\rho_f$  and  $\rho_p$  are the fiber and polymer density, respectively.

Five hollow fibers with the length of 50 cm were dried for 2 h at 105 °C in a vacuum oven and weighed. The fiber density was calculated from the mass to volume ratio as:

$$\rho_f = \frac{4w}{\pi(d_o^2 - d_i^2)L} \quad (2)$$

Where L is the fiber length (cm); w is the fibers mass (gr);  $d_i$  is the inner diameter and  $d_o$  is the outer diameter (cm) of the hollow fibers.

In this study, mean pore size and effective surface porosity were estimated using N<sub>2</sub> permeation test. Total gas permeation rate through a porous asymmetric membrane can be assumed on the basis of the combination of Poiseuille and Knudsen flows [26]. By assuming cylindrical pores in the outer skin layer of the asymmetric membrane, the gas permeance can be calculated as the following equation [27, 28]:

$$J_A = \frac{2r_p \varepsilon}{3RT L_p} \left( \left( \frac{8RT}{\pi M} \right)^{0.5} \right) + \frac{r_p^2}{8\mu RT L_p} \varepsilon \bar{P} \quad \text{or} \quad J_A = K_0 + P_0 \bar{P} \quad (3)$$

Where  $J_A$  is the gas permeance (mol/m<sup>2</sup> s Pa);  $r_p$  and  $L_p$  are pore radius and effective pore length, respectively (m);  $\varepsilon$  is surface porosity; R is universal gas constant 8.314 (J/mol K);  $\mu$  is gas viscosity (kg/m s); M is gas molecular weight (Kg/mol); T is gas temperature (K); and  $\bar{P}$  is mean pressure (Pa).

According to Eq.(3), by plotting  $J_A$  versus mean pressure, mean pore size and effective surface porosity over the pore length,  $\varepsilon/L_P$ , can be calculated from the intercept ( $K_0$ ) and slope ( $P_0$ ) of the obtained line, as the following:

$$r_p = 5.33 \left( \frac{P_0}{K_0} \right) \left( \frac{8RT}{\pi M} \right)^{0.5} \mu \quad (4)$$

$$\frac{\varepsilon}{L_P} = \frac{8\mu RT P_0}{r_p^2} \quad (5)$$

As for the contact angle measurement, samples of the hollow fibers were dried in a vacuum oven at  $60 \pm 2$  °C for 12 h. The sessile drop technique using a goniometer (model G1, Krüss GmbH, Hamburg, Germany) was applied to measure the contact angle of the outer surface of the hollow fibers. The contact angle values of each sample were measured at ten various positions of the sample and then averaged.

Pure water flux of the membranes was measured to evaluate the membrane performance. In this experiment, the membrane module was pressurized from 100 up to 700 kPa. The water flux ( $J_w$ ) was calculated as below:

$$J_w = V / A \cdot \Delta t \quad (6)$$

Where  $J_w$  is water flux ( $L/m^2$  hr);  $V$  is the volume of permeate collected (L);  $\Delta t$  is the sampling time (h); and  $A$  is the membrane area ( $m^2$ ).

Pure water flux of the membranes as a function of the trans-membrane pressure (TMP) was measured to determine the membrane hydraulic resistance ( $R_m$ ). Using the slope of water flux vs. TMP graph, the hydraulic resistance of the membrane was evaluated as the following equation [29]:

$$J_w = \Delta P / R_m \quad (7)$$

In order to conduct oil–water separation, oil–water emulsion was prepared by adding 500 mg of kerosene into 1000 ml of distilled water under constant stirring (5000 rpm). The resulting stable emulsion had oil droplets in the range of 0.5–1  $\mu m$  that was estimated using optical microscope (BHS-323, OLYMPUS Co., Ltd., Tokyo, Japan). After preparing the membrane modules, a cross-flow experimental set-up was used for the oil–water separation, as shown in Figure 1. Parameters of the module prepared are given in Table 3. The permeate side was open to the atmosphere and the TMP was controlled using the by-pass valve of the pump. The flow rate in the shell side of the module was adjusted by the flow control valve manually. The permeate volume collected was used to measure the permeate flux. Also, in order to minimize the penetration of oil through the membrane pores, the ultrafiltration of oil-water emulsion was conducted at low transmembrane pressure of 400 Kpa. A high liquid flowrate of 200 ml/min through the shell side of the module was used for the reduction of fouling. Oil concentrations in the feed and permeate were measured using a TOC (total

organic carbon) analyser (GE Analytical Instrument 500RL). The percentage of oil rejection for the membrane was calculated by the following equation [30]:

$$f(\%) = \left(1 - \frac{C_p}{C_f}\right) \times 100 \quad (8)$$

Where  $f$  is the rejection,  $C_p$  and  $C_f$  (mg/l) are the concentration of permeate and the feed, respectively.

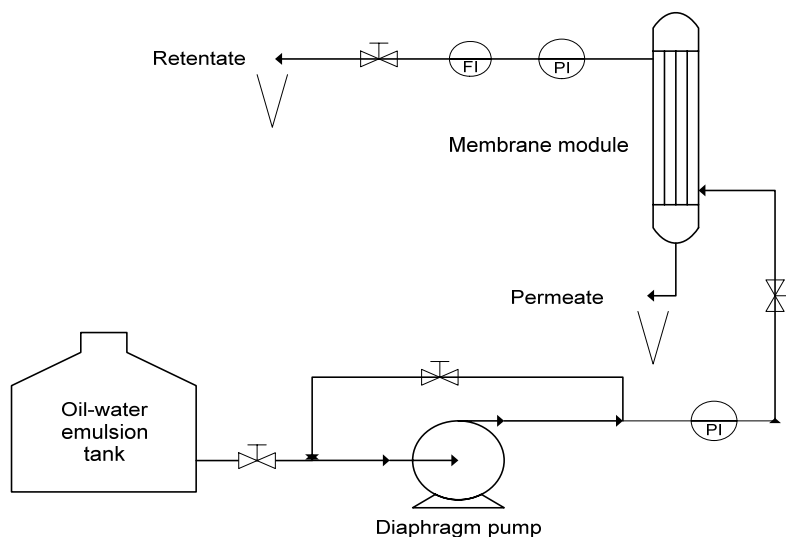


Figure1. Schematic of experimental ultrafiltration system

Table 3. The membrane module parameters

Module inner diameter (mm)	14
Module length (mm)	280
Effective fiber length (mm)	180
Fiber outer diameter (mm)	0.7
Fiber inner diameter (mm)	0.35
No. of fibers	20

### 3. Results and Analysis

#### 3.1. Morphological analysis of the membranes

Cross-section, inner surface and outer surface morphology of the plain PSF membrane are given in Figure 2. As can be seen, because of a fast phase-inversion process, large cavities appeared in the cross-section of the membrane. The spongy sublayer was generated due to the delay phase-inversion from the bore side. Since an aqueous solution of 70% NMP was used as the bore fluid, the delay solidification resulted in an inner skinless layer. The outer skin of the membrane had small nano pore sizes which could not be visible at 5K magnification.

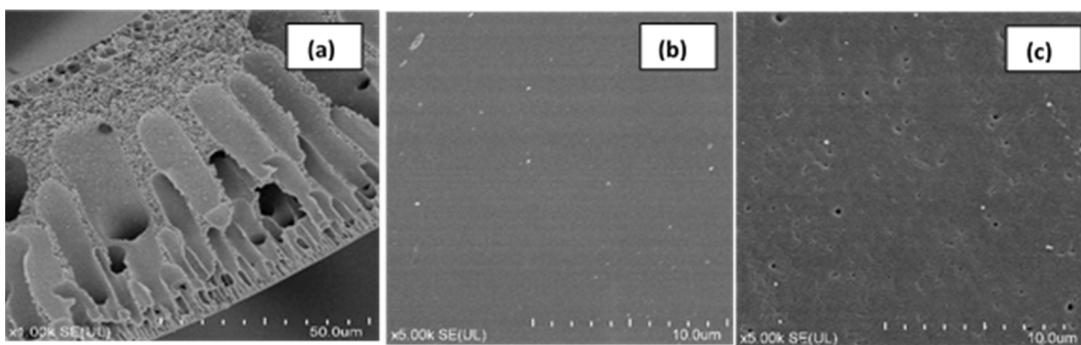


Figure 2. SEM micrographs of plain PSF membrane: (a) cross-section; (b) outer surface; and (c) inner surface

Figure 3 shows the morphological structure of the prepared blend PSF-SPEEK hollow fiber membrane. It should be noted that the morphology of asymmetric membranes is controlled by thermodynamic and kinetic effects of the phase-inversion process [31]. By addition of SPEEK, the cavities in the cross-section of the membrane became larger and the spongy area decreased. Viscosity is considered as the kinetic effect that influences mutual diffusion of solvent (in the polymer solution) and non-solvent (in the coagulation bath) during the phase-inversion process. In fact, by addition of SPEEK, thermodynamic stability of the solution decreased which resulted in a fast phase-inversion and the generation of large finger-like structure. In this case, it seems that the kinetic effect is overtaken by the thermodynamic effect. In addition, by increasing the viscosity of the blend solution, a delay phase-inversion from the outer surface resulted in a thicker skin layer. Therefore, the outer surface seems to have smaller pore size and porosity which can be confirmed by the results of  $N_2$  permeation test in the following section. The inner skinless surface was produced due to using a weak non-solvent (70% NMP) as the bore fluid.

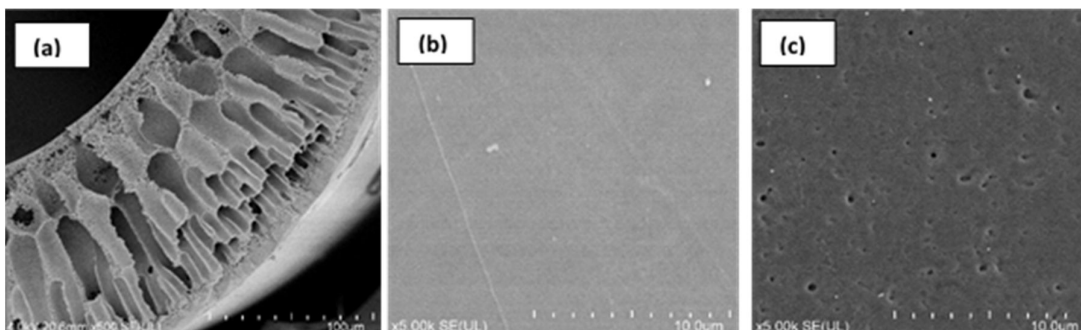


Figure 3. SEM micrographs of blend PSF-SPEEK membrane: (a) cross-section; (b) outer surface; and (c) inner surface

### 3.2 Properties of the prepared hollow fiber membranes

Mean pore size and effective surface porosity of the prepared membranes were estimated using the  $N_2$  permeation test. Figure 4 shows  $N_2$  permeance of the membranes as a function of the mean pressure.

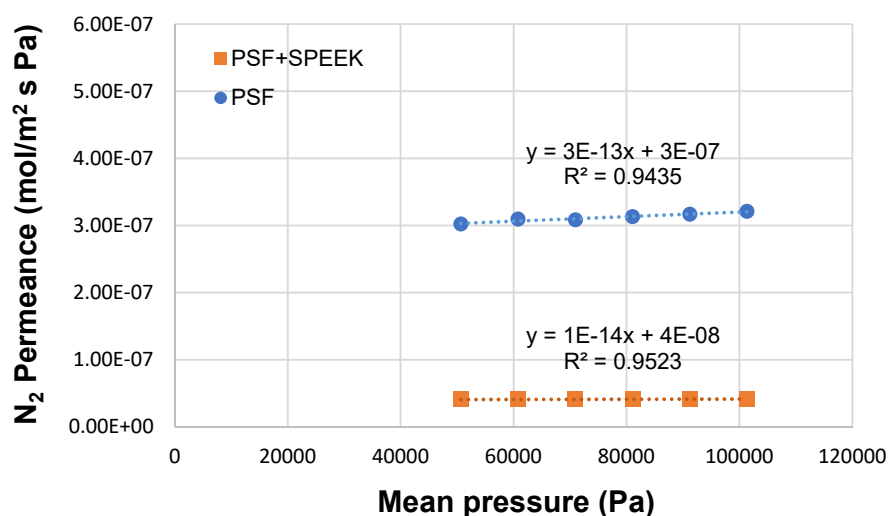


Figure 4. N<sub>2</sub> permeance of the hollow fiber membranes as the function of mean pressure

As mentioned in the preceding section, by obtaining the intercept and slope of the lines plotted in Figure 4 the mean pore size and the effective surface porosity were calculated. The results are given in Table 4. From Figure 4, N<sub>2</sub> permeance of the PSF-SPEEK membrane remained almost constant by increasing the mean pressure. This phenomenon indicates that the Knudsen flow controls gas transport through the membrane pores which confirms the small size pores of the membrane. Furthermore, the blend membrane with thick outer skin layer showed lower permeability and surface porosity.

Table 4. Properties of the hollow fiber membranes

Membrane	N <sub>2</sub> permeation 100 kPa (GPU)	Mean pore size (nm)	surface porosity ( $\epsilon/L_p$ )(m <sup>-1</sup> )	Hydraulic resistance (m <sup>2</sup> h bar/L)	Water contact angle (°)	Overall porosity (%)
PSF	1010	90	52	3.24	72.2±0.6	74.6
PSF+SPEEK	134	22	28	0.483	63.8±4.4	78.8

The Hydrophilicity of the prepared membranes was measured by a water contact angle measurement. As shown in Table 4, by addition of SPEEK in the PSF solution, the prepared membrane presented a significantly lower contact angle value (63.8°). Since SPEEK is a highly hydrophilic material (possessing sulfone groups), the decrease in the contact angle of blend PSF-SPEEK membranes can be related to the nature of SPEEK. In fact, increasing the hydrophilicity can result in the improvement of water flux of the membrane.

The overall porosity of the prepared hollow fiber membranes is shown in Table 4. Since overall porosity represents the void fraction of the membrane structure, the membrane morphology plays an important role in the porosity value. It can be seen that by addition of SPEEK the overall porosity of the membrane relatively increased which can be associated to the generated open finger-like structure. Meanwhile, the plain PSF membrane presented a more dense structure with the lower overall porosity.

The water flux of the membranes as a function of TMP is plotted in Figure 5. The slope of the lines was used to estimate the hydraulic resistance of the

membranes (Table 4). As shown in Figure 5, a significant increase in water flux was observed for the blend membrane by increasing TMP. This can be related to the enhanced hydrophilicity and the open structure (finger-like) of the blend PSF-SPEEK membrane. A similar water flux improvement was reported for the blend PAN membranes when using the hydrophilic surfactant of IGEPAL in the polymer dope [32]. Due to the improved structure of the blend membrane, the hydraulic resistance of the blend membrane significantly reduced.

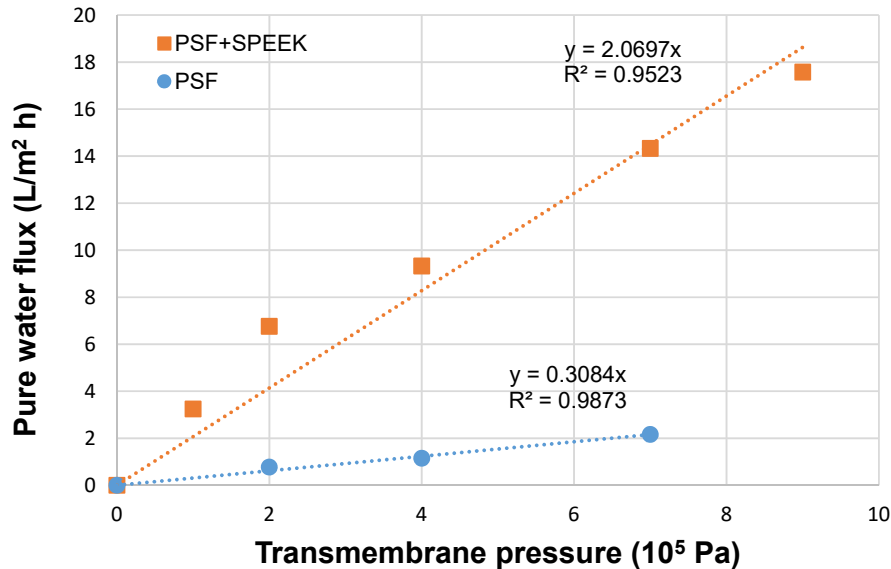


Figure 5. Pure water flux of the hollow fiber membranes as the function of transmembrane pressure ( $Q_L=200$  ml/min; and  $T=25$  °C)

### 3.3. Oil-water separation performance

In order to evaluate the separation performance of the membranes, oil rejection test was conducted through the cross-flow membrane separation system at constant pressure of 400 kPa and flow rate of 200 ml/min. The results of oil rejection as a function of operating time are shown in the Figure 6. The oil rejection increased as a function of time due to the formation of cake layer as an extra filtration layer [33]. A stable oil rejection of over 98 % was achieved for the blend PSF-SPEEK hollow fiber membrane with smaller pore sizes. The plain PSF membrane presented an approximate rejection of 90 % which can be related to the outer surface morphology with larger pore sizes. Despite the fact that the mean pore size of both membranes are smaller than the oil droplets, a small amount of the oil is still present in the permeate side. This incomplete rejection can be related to the concentration of oil droplets at the outer surface of the membranes. In fact, at high pressure, concentration polarization can result in the penetration of oil through the membrane [34].

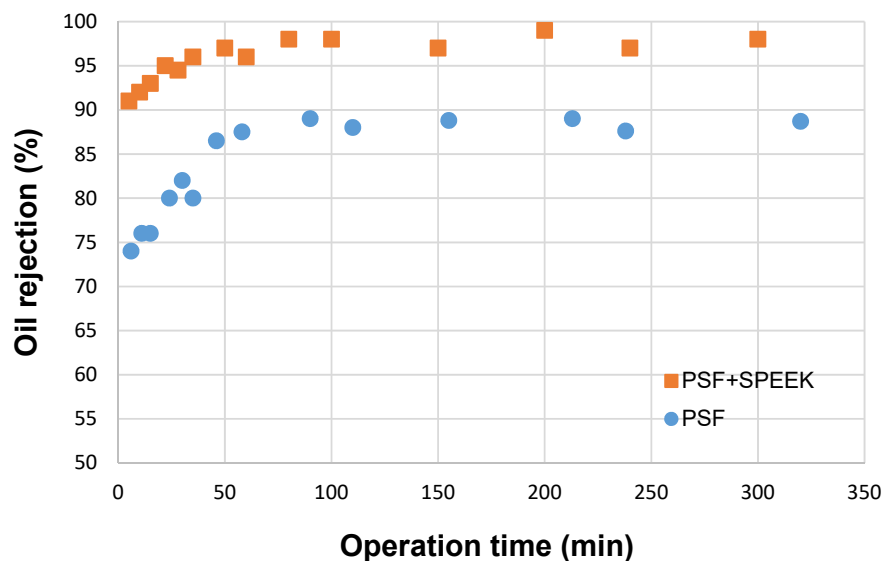


Figure 6. Oil rejection performance of the hollow fiber membranes as the function of operation time ( $\Delta P = 400$  kPa;  $Q_L = 200$  ml/min; and  $T = 25$  °C)

Figure 7 displays the water permeate flux of the prepared hollow fiber membranes during the oil-water separation experiment. The membranes showed a gradual permeate flux reduction which can be attributed to the formation of a cake layer and the fouling of the membranes. As the cake layer builds up, the mass transfer resistance to the permeation process certainly increases, which results in a drop in the permeate flux [35]. In a similar study Zhu et al. [36], indicates to an initial significant flux reduction due to the immediate formation of an oil layer and after that the flux decreased slowly caused by the formation of a stable dynamic oil layer with approximately constant thickness. In addition, the compressibility or porosity of the cake layer can affect the separation performance [37]. The openings in the cake layer can be associated to the nature of the foulants, in which a denser cake layer is more inconvenient to the permeate flux. As shown in Figure 7, after about 100 min of the operation, the flux of the blend PSF-SPEEK reduced from  $9 \text{ L/m}^2 \text{ h}$  to about  $6.5 \text{ L/m}^2 \text{ h}$ . Meanwhile, the plain PSF membrane showed a flux reduction from  $1.1 \text{ L/m}^2 \text{ h}$  to about  $0.6 \text{ L/m}^2 \text{ h}$  during 60 min of the operation. It can be said that the rate of decreasing flux for the blend membrane is relatively lower than the plain PSF membrane. This reveals that the fouling rate of the blend PSF-SPEEK membrane is lower than the plain PSF membrane which can be related to the blend membrane structure with higher degree of hydrophilicity.

Therefore, the improvement of the membrane structure with narrow pore size distribution, high hydrophilicity and low resistance can enhance the oil rejection and the permeation flux which form the main parameters to commercialize the technology.

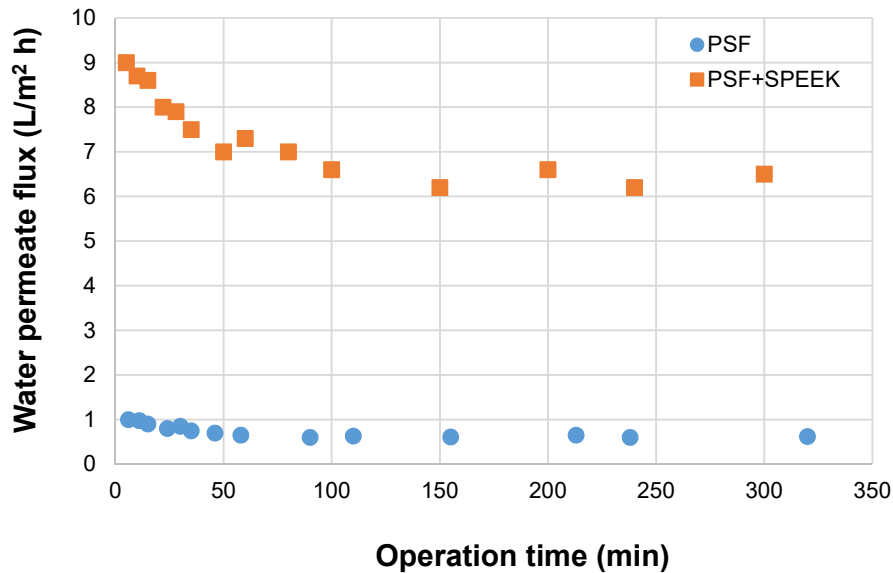


Figure 7. Permeate flux of the hollow fiber membranes as the function of operation time ( $\Delta P=400$  kPa;  $Q_L=200$  ml/min; and  $T=25$  °C)

#### 4. Conclusion

SPEEK was introduced into the PSF solution in order to enhance the hydrophilicity and the membrane structure for the oil–water separation. The prepared membranes were characterized in terms of morphology, pore size, hydrophilicity, water flux, hydraulic resistance and oil rejection. By addition of SPEEK, the blend membrane presented a finger-like morphology with a thicker outer skin layer and smaller pore sizes. The blend membrane showed the overall porosity of 78.8% due to the open structure. Outer surface water contact angle of the blend hollow fiber membrane decreased from  $72^\circ$  to about  $64^\circ$  due to the addition of hydrophilic SPEEK in the solution. From  $N_2$  permeation test, the PSF-SPEEK blend membrane showed lower permeability and mean pore size. The PSF-SPEEK membrane has  $N_2$  permeance of 134 GPU and mean pore size of 22 nm. The blend membrane showed higher pure water flux ( $9.3$  L/m<sup>2</sup> h) and lower hydraulic resistance ( $0.483$  m<sup>2</sup> h bar/L) due to the higher hydrophilicity and the produced open structure. Oil rejection of over 98% and a stable water permeate flux of  $6.5$  L/m<sup>2</sup> h were achieved for the blend membrane due to the improved structure with small pore sizes and good hydrophilicity.

#### Nomenclature

A	Membrane area (m <sup>2</sup> )
$C_f$	Feed concentration (mg/l)
$C_p$	Permeate concentration (mg/l)
$d_i$	Inner diameter of hollow fiber (cm)
$d_o$	Outer diameter of hollow fiber (cm)
f	Oil rejection (%)
$J_A$	Gas permeance (mol/m <sup>2</sup> s Pa)
$J_w$	Water flux (L/m <sup>2</sup> hr)

M	Gas molecular weight (Kg/mol)
L	Fiber length (cm)
$L_p$	Pore length (m)
R	Gas constant 8.314 (J/mol K)
$R_m$	Membrane hydraulic resistance ( $m^2$ h bar/L)
$r_p$	Pore radius (m)
T	Gas temperature (K)
V	Permeate volume (L)
W	Fibers mass (gr)
$\epsilon$	Membrane surface porosity (-)
$\epsilon_m$	Membrane overall porosity (%)
$\mu$	Gas viscosity (kg/m s)
$\rho_f$	Fiber density ( $gr/cm^3$ )
$\rho_p$	Polymer density ( $gr/cm^3$ )
$\bar{P}$	Mean pressure (Pa)
$\Delta P$	Pressure difference (Pa)
$\Delta t$	Sampling time (h)

## References

- [1] J. Kong, K. Li. "Oil removal from oil-in-water emulsions using PVDF membranes." *Sep. Purif. Technol.*, vol. 16, pp. 83–93, 1999.
- [2] T. Mohammadi, A. Pak, M. Karbassian, M. Golshan. "Effect of operating conditions on microfiltration of an oil-water emulsion by a kaolin membrane." *Desalination*, vol. 168, pp. 201–205, 2004.
- [3] A. Salahi, T. Mohammadi, R. Mosayebi Behbahani, M. Hemmati. "Asymmetric polyethersulfone ultrafiltration membranes for oily wastewater treatment: Synthesis, characterization, ANFIS modeling, and performance." *J. Environ. Chem. Eng.*, vol. 3, pp. 170–178, 2015.
- [4] J. Cui, X. Zhang, H. Liu, S. Liu, K.L. Yeung. "Preparation and application of zeolite/ceramic microfiltration membranes for treatment of oil contaminated water." *J. Membr. Sci.*, vol. 325, pp. 420–426, 2008.
- [5] D. Wandera, S.R. Wickramasinghe, S.M. Husson. "Modification and characterization of ultrafiltration membranes for treatment of produced water." *J. Membr. Sci.*, vol. 373, pp.178–188, 2011.
- [6] U. Daiminger, W. Nitsch, P. Plucinski, S. Hoffmann. "Novel techniques for oil/water separation." *J. Membr. Sci.*, vol. 99, pp.197–203, 1995.
- [7] R.S. Faibish, Y. Cohen. "Fouling and rejection behaviour of ceramic and polymer-modified ceramic membranes for ultrafiltration of oil-in-water emulsions and microemulsions." *Colloid Surf. A: Physicochem Eng. Asp.*, vol 191, pp. 27–40, 2001.
- [8] G. Gutiérrez, A. Lobo, J.M. Benito, J. Coca, C. Pazos. "Treatment of a waste oil-in-water emulsion from a copper-rolling process by ultrafiltration and vacuum evaporation." *J. Hazard. Mater.*, vol. 185, pp.1569–1574, 2011.

- [9] B. Tansel, J. Regula, R. Shalewitz. "Treatment of fuel oil and crude oil contaminated waters by ultrafiltration membranes." *Desalination*, vol. 102, pp. 301–311, 1995.
- [10] J.M. Benito, M.Z. Sanchez, P. Pena, M.A. Rodriguez. "Development of a new high porosity ceramic membrane for the treatment of bilge water." *Desalination*, 214, pp.91–101, 2007.
- [11] L. Giorno, R. Mazzei, M. Oriolo, G. De Luca, M. Davoli, E. Drioli. "Effects of organic solvents on ultrafiltration polyamide membranes for the preparation of oil-in-water emulsions." *J. Colloid Interface Sci.*, vol. 287, pp.612–623, 2005.
- [12] T. Jin, J. Song, J. Zhu, L.D. Nghiem. "The role of the surfactant sodium dodecyl sulfate to dynamically reduce mass transfer resistance of SPEEK coated membrane for oil-in-water emulsion treatment." *J. Membr. Sci.*, vol. 541, pp. 9–18, 2017.
- [13] C. Wu, A. Li, L. Li, L. Zhang, H. Wang, X. Qi, Q. Zhang. "Treatment of oily water by a poly(vinyl alcohol) ultrafiltration membrane." *Desalination*, vol. 225, pp. 312–321, 2008.
- [14] N.M. Kocherginsky, C.L. Tan, W.F. Lu. "Demulsification of water in- oil emulsions via filtration through a hydrophilic polymer membrane." *J. Membr. Sci.*, vol. 220, pp.117–128, 2003.
- [15] L. Li, L. Ding, Z. Tu, Y. Wan, D. Clause, J.L. Lanoisellé. "Recovery of linseed oil dispersed within an oil-in-water emulsion using hydrophilic membrane by rotating disk filtration system." *J. Membr. Sci.*, vol. 342, pp.70–79, 2009.
- [16] J. Zhoua, Q. Changa, Y. Wang, J. Wang, G. Meng. "Separation of stable oil–water emulsion by the hydrophilic nano-sized ZrO<sub>2</sub> modified Al<sub>2</sub>O<sub>3</sub> microfiltration membrane." *Sep. Purif. Technol.*, vol. 75, pp. 243–248, 2010.
- [17] B. Chakrabarty, A.K. Ghoshal, M.K. Purkait. "Cross-flow ultrafiltration of stable oil-in-water emulsion using polysulfone membranes." *Chem. Eng. J.*, vol. 165, pp. 447–456, 2010.
- [18] B. Chakrabarty, A.K. Ghoshal, M.K. Purkait. "Ultrafiltration of stable oil-in-water emulsion by polysulfone membrane." *J. Membr. Sci.*, vol. 325, pp.427–437, 2008.
- [19] W. Chen, Y. Su, L. Zheng, L. Wang, Z. Jiang. "The improved oil/water separation performance of cellulose acetate-graft-polyacrylonitrile membranes." *J. Membr. Sci.*, vol. 337, pp. 98-105, 2009.
- [20] K. Zhu, S. Zhang, J. Luan, Y. Mu, Y. Du, G. Wang. "Fabrication of ultrafiltration membranes with enhanced antifouling capability and stable mechanical properties via the strategies of blending and crosslinking." *J. Membr. Sci.*, vol. 539, pp. 116–127, 2017.

- [21] J. Saadati, M. Pakizeh. "Separation of oil/water emulsion using a new PSf/pebax/F-MWCNT nanocomposite membrane." *J. Taiwan Ins. Chem. Eng.*, vol. 71, pp. 265–276, 2017.
- [22] Y. Gao, Z. Li, B. Cheng, K. Su. "Superhydrophilic poly(p-phenylene sulfide) membrane preparation with acid/alkali solution resistance and its usage in oil/water separation." *Sep. Purif. Technol.*, vol. 192, pp. 262-270, 2018.
- [23] J-H Zuo, P. Cheng, X-F Chen, X. Yan, Y-J Guo, W-Z Lang. "Ultra-high flux of polydopamine-coated PVDF membranes quenched in air via thermally induced phase separation for oil/water emulsion separation." *Sep. Purif. Technol.*, vol. 192, pp. 348-359, 2018.
- [24] A.F. Ismail, I.R. Dunkinb, S.L. Gallivanb, S.J. Shilton. "Production of super selective polysulfone hollow fiber membranes for gas separation." *Polymer*, vol. 40, pp. 6499–6506, 1999.
- [25] F. Tasselli, J.C. Jansen, F. Sidari, E. Drioli. "Morphology and transport property control of modified poly (ether ether ketone) (PEEKWC) hollow fiber membranes prepared from PEEKWC/PVP blends: influence of the relative humidity in the air gap." *J. Membr. Sci.*, vol. 255, pp. 13–22, 2005.
- [26] J.M.S. Henis, M.K. Tripodi. "Composite hollow fiber membranes for gas separation: the resistance model approach." *J. Membr. Sci.*, vol. 8, pp. 233–46, 1981.
- [27] A. Mansourizadeh, S. Mousavian. "Structurally developed microporous polyvinylidene fluoride hollow-fiber membranes for CO<sub>2</sub> absorption with diethanolamine solution." *J. Polym. Res.*, vol. 20, n. 99, pp. 1–12, 2013.
- [28] A. Mansourizadeh, A.F. Ismail, T. Matsuura. "Effect of operating conditions on the physical and chemical CO<sub>2</sub> absorption through the PVDF hollow fiber membrane contactor." *J. Membr. Sci.*, vol. 353, pp. 192–200, 2010.
- [29] R. Mahendran, R. Malaisamy, D.R. Mohan. "Cellulose acetate and polyethersulfone blend ultrafiltration membranes. Part I: preparation and characterizations." *Polym. Adv. Technol.*, vol. 15, pp. 149–157, 2004.
- [30] A. Mansourizadeh, A. Javadi Azad. "Preparation of blend polyethersulfone/cellulose acetate/polyethylene glycol asymmetric membranes for oil–water separation." *J. Polym. Res.*, vol. 21, n. 375, pp. 1-9, 2014.
- [31] E. Fontananova, J.C. Jansen, A. Cristiano, E. Curcio, E. Drioli. "Effect of additives in the casting solution on the formation of PVDF membranes." *Desalination*, vol. 192, pp.190–197, 2006.
- [32] E. Shekarian, E. Saljoughi, A. Naderi. "Polyacrylonitrile (PAN)/IGEPAL blend asymmetric membranes: preparation, morphology, and performance." *J. Polym. Res.*, vol. 20, n. 162, pp.1–9, 2013.

- [33] R.S. Faibish, Y. Cohen. "Fouling-resistant ceramic-supported polymer membranes for ultrafiltration of oil-in-water microemulsions." *J. Membr. Sci.*, vol. 185, pp.129–143, 2001.
- [34] P. Lipp, C.H. Lee, A.G. Fane, C.J.D. Fell. "A fundamental study of the ultrafiltration of oil-water emulsions." *J. Membr. Sci.*, vol. 36, pp.161–177, 1988.
- [35] J. Mendret, C. Guigui, P. Schmitz, C. Cabassud. "In situ dynamic characterisation of fouling under different pressure conditions during dead-end filtration: compressibility properties of particle cakes." *J. Membr. Sci.*, vol. 333, pp. 20–29, 2009.
- [36] L. Zhu, M. Chen, Y. Dong, C.Y. Tang, A. Huang, L. Li. "A low-cost mullite-titania composite ceramic hollow fiber microfiltration membrane for highly efficient separation of oil-in-water emulsion." *Water Res.*, vol. 90, pp. 277–285, 2016.
- [37] J. Li, V.Y. Hallbauer-Zadorozhnaya, D.K. Hallbauer, R.D. Sanderson. "Cake-layer deposition, growth, and compressibility during microfiltration measured and modeled using a noninvasive ultrasonic technique." *Ind. Eng. Chem. Res.*, vol. 41, pp. 4106–4115, 2002.

## ساخت غشاهای اولترافیلتراسیون آبدوست و مخلوطی پلی سولفون - پلی اتر کتون سولفون شده برای تصفیه پساب های روغنی

امیر منصوری زاده\*، مهرسا محمدی

ایران، گچساران، دانشگاه آزاد اسلامی واحد گچساران، گروه مهندسی شیمی

### مشخصات مقاله

تاریخچه مقاله:

دریافت: ۱۰ آبان ۱۳۹۷  
پذیرش نهایی: ۴ دی ۱۳۹۷

کلمات کلیدی:

غشای مخلوطی پلی سولفون  
پلی اتر کتون سولفون شده  
پس زنی روغن  
تصفیه پساب

\* عهده دار مکاتبات؛

رایانامه:

a.mansourizadeh@yahoo.com

تلفن: +۹۸ ۹۱۷۸۵۰۸۳۷۳

دورنگار: +۹۸ ۷۴ ۳۲۳۳۲۰۳۳

### چکیده

جداسازی غشایی یکی از روشهای موثر برای تصفیه پساب های روغنی می باشد. در این تحقیق بمنظور افزایش آبدوستی و بهبود ساختار غشاها جهت جداسازی آب-روغن، پلی اتر کتون سولفون شده (SPEEK) به محلول پلی سولفون (PSF) اضافه شده است. غشاهای الیاف توخالی با یک فرآیند جداسازی فازی تهیه شده اند. غشاها با آزمون های تراوایی نیتروژن، زاویه تماس با آب، شار آب خالص و میکروسکپ الکترونی روبشی مشخصه بندی شده اند. غشای مخلوطی PSF-SPEEK مورفولوژی بندانگشتی با پوسته سطحی ضخیمتر و حفره های سطحی کوچکتر نشان دادند. بدلیل ساختار باز تولید شده، غشای مخلوطی تخلخل کلی ۷۷/۸٪ نشان داد. بدلیل ماهیت آبدوست SPEEK زاویه تماس سطحی غشای مخلوطی ۸ درجه کاهش نشان داده است. غشای مخلوطی دارای تراوایی نیتروژن GPU ۱۳۴ و اندازه متوسط حفره سطحی ۲۲ نانومتر می باشد. شار آب خالص  $9/3 \text{ L/m}^2 \text{ h}$  در فشار ۴ بار و مقاومت هیدرولیکی  $0/483 \text{ m}^2 \text{ h bar/L}$  برای غشای مخلوطی آبدوست بدست آمده است. در تست جداسازی آب-روغن، غشای مخلوطی بهینه دارای درصد پس زنی روغن ۹۸٪ و تراوایی آب  $6/5 \text{ L/m}^2 \text{ h}$  می باشد که مربوط به حفره های کوچک سطحی و افزایش آبدوستی بوده است.